# EEG Correlation of the Discharge Properties of Identified Neurons in the Basal Forebrain

A. DUQUE,[1] B. BALATONI,[2] L. DETARI,[2] AND L. ZABORSZKY[1]

[1]*Center for Molecular and Behavioral Neuroscience, Rutgers, The State University of New Jersey, Newark, New Jersey 07102; and* [2]*Department of Comparative Physiology, Eotvos Lorand University, H-1088 Budapest, Hungary*

**Duque, A., B. Balatoni, L. Detari, and L. Zaborszky.** EEG correlation of the discharge properties of identified neurons in the basal forebrain. *J Neurophysiol* 84: 1627–1635, 2000. The basal forebrain (BF) is a heterogeneous structure located in the ventral aspect of the cerebral hemispheres. It contains cholinergic as well as different types of noncholinergic corticopetal neurons and interneurons, including GABAergic and peptidergic cells. The BF constitutes an extrathalamic route to the cortex, and its activity is associated with an increase in cortical release of the neurotransmitter acetylcholine, concomitant with electroencephalographic (EEG) low-voltage fast activity (LVFA). However, the specific role of the different BF cell types has largely remained unknown due to the lack of chemical identification of the recorded neurons. Here we show that the firing rate of immunocytochemically identified cholinergic and parvalbumin-containing neurons increase during cortical LVFA. In contrast, increased neuropeptide Y neuron firing is accompanied by cortical slow waves. Our results, furthermore, indicate that BF neurons posses a distinct temporal relationship to different EEG patterns and suggest a more dynamic interplay within BF as well as between BF and cortical circuitries than previously proposed.

## INTRODUCTION

Basal forebrain (BF) areas, including the substantia innominata (SI), pallidal regions (ventral pallidum and globus pallidus), vertical (VDB) and horizontal (HDB) limbs of the diagonal band and the medial septum contain a heterogeneous population of neurons, including cholinergic, GABAergic projection neurons and putative interneurons (Gritti et al. 1993; Zaborszky et al. 1999). Single-unit recordings in the BF in combination with electroencephalographic (EEG) monitoring in anesthetized animals as well as during various behaviors indicated that BF inputs to the neocortex are important in neocortical activation (Buzsaki et al. 1988; Detari et al. 1999; Jimenez-Capdeville et al. 1997; Metherate et al. 1992; Nunez 1996). However, the cellular mechanism of how the BF modulates cortical activation remained largely obscure due to the fact that these studies did not identify the recorded neurons chemically or morphologically (Detari et al. 1999; Pang et al. 1998).

In urethan anesthesia, several distinct EEG patterns can appear depending on the level of anesthesia (Detari et al. 1997; Grahn et al. 1989). For example, under light anesthesia, periods with low-voltage fast activity (LVFA) alternate with epochs of slow waves (SWA) at a frequency of ~0.1–0.3 Hz (pattern I, Fig. 1*A*). Under deeper anesthesia, another characteristic pattern (pattern II, Fig. 1*B*) appears, in which deep-positive inactive periods and short activations riding on deep-negative deflections alternate at a rate <1 Hz. This slow rhythm, first described by Steriade et al. (1993), is transformed into "burst-suppression" pattern by the deepening of the anesthesia. During the continuous transition, inactive periods become longer and rhythmicity is lost (Korkmaz and Wahlstrom 1997; Steriade et al. 1994). Slow rhythm can be observed during natural sleep, and it is probably generated by the same mechanisms as in anesthesia.

The purpose of this study was to record extracellular single-unit activity in the BF that was related to these cortical EEG epochs in urethan-anesthetized rats and subsequently determine the transmitter content of the recorded neurons by using the juxtacellular labeling method of Pinault (1996) in combination with immunostaining for choline acetyltransferase (ChAT), parvalbumin (PV), and neuropeptide Y (NPY).

## METHODS

### Animals and electrophysiology

All procedures were carried out in strict accordance with guidelines set forth in the Public Health Service manual "Guide for the Use and Care of Laboratory Animals." Male Sprague Dawley rats (250–350 g; Zivic Miller Laboratories, Portersville, PA) were anesthetized with urethan (1.2 g/kg ip, supplemented later as necessary) and placed in a stereotaxic apparatus with bregma and lambda leveled. All wound margins and points of contact between the animal and the stereotaxic apparatus were infiltrated with lidocaine solution (2%) and xylocaine ointment (5%), respectively. Body temperature was kept at 37°C with an electric heating pad. The scalp and overlying fascia were retracted from the skull and small burr holes were drilled, in both hemispheres, over the prefrontal/frontal cortex for EEG recordings [Anteroposterior (AP) +2.0–4.0 mm, lateral (L) ±0.5–2.0, relative to bregma] and over the BF [AP −0.3-(−1.0), L ±2.4–3.2 mm, relative to bregma] for single-unit recordings. Simultaneous cortical EEG and single-cell extracellular recordings from different BF areas including the HDB, the SI and the globus pallidus (GP), were obtained. Recording electrodes were constructed from 2.0-mm-OD borosilicate glass capillaries (World Precision Instruments, Sarasota, FL) on a Narishige PE-2 (Narishige, Tokyo, Japan) vertical pipette puller. The tips of the electrodes were broken under visual guidance to approximately 0.5–
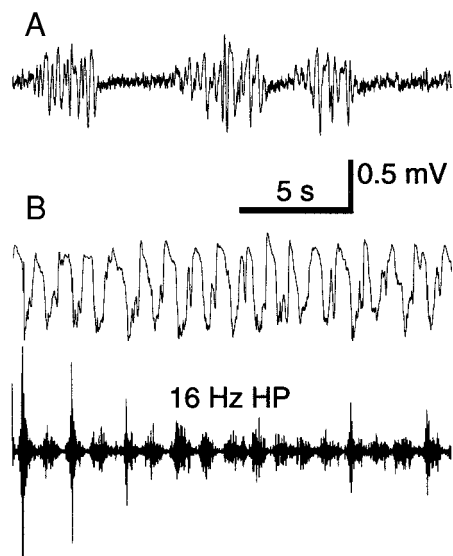
FIG. 1. Examples of 2 basic electroencephalographic (EEG) patterns recorded under urethan anesthesia in rat. *A*: EEG pattern I. Low-voltage fast activity (LVFA) alternates with epochs of slow waves at frequencies of ~0.1–0.3 Hz under the lightest level of anesthesia. *B, top*: EEG pattern II. This pattern, in which slow wave activity predominates, is caused by deeper anesthesia. *Bottom*: the same EEG pattern II period filtered with a high pass filter at 16 Hz to illustrate the location of high frequencies in the deep negative components of this pattern. In this and all subsequent EEG records deep positive is up. Scale bars apply to both *A* and *B*.

1.5 $\mu$m in diameter, and they had in vitro impedances of 15–25 M$\Omega$ when filled with 0.5 M NaCl containing 5% biocytin. Following extracellular recordings, neurons were juxtacellularly labeled by applying 2- to 10-nA, 200-ms current pulses for 8–20 min using an IR-183 Neurodata amplifier (Neurodata Instruments, New York, NY). Transcortical EEG recording electrodes consisted of bipolar stainless steel enamel coated wires (California Fine Wire, Grover Beach, CA) approximately 100 $\mu$m in diameter. The superficial electrode touched the pial surface, while the deep one was located in the pyramidal layer. Both, EEG and single-unit signals were simultaneously amplified, filtered, and recorded using standard equipment.

### Perfusion

Animals were perfused with 150 ml saline followed first by 200 ml of 4% paraformaldehyde, 15% picric acid, and 0.5% glutaraldehyde (GA) and then by 200 ml of the same fixative without the GA. Brains were postfixed overnight in the second fixative.

### Immunocytochemistry

Coronal sections 50-$\mu$m thick were cut through the BF with a Vibratome®. Sections were incubated overnight in avidin conjugated lissamine rhodamine (LR) (1:500; Jacson ImmunoResearch Labs, West Grove, PA). The recorded and biocytin filled (LR+) neuron was found using an epifluorescent microscope. Stained somas were sequentially immunostained for the presence of ChAT followed by PV and NPY. For ChAT a monoclonal rat anti-ChAT antibody was used (Rat anti-choline acetyltranferase; 1:10; 2 overnights at 4°C; Boehringer Mannheim, Mannheim, Germany). For PV and NPY rabbit polyclonal antibodies were used (Rabbit anti-PV; 1:1000; 2 overnights at 4°C; kindly provided by Dr. K. Baimbridge, Vancouver, Canada. Rabbit anti NPY; 1:500; 2 overnights at 4°C; Peninsula Laboratories, Belmont, CA). Visualization of ChAT, PV, and NPY was done with a secondary antibody conjugated to fluorescein isothiocyanate (FITC) (FITC conjugated goat anti rat/rabbit; 1:100; 4 h at RT; Jacson ImmunoResearch Labs, West Grove, PA). Finally, the

LR+ somas were developed for light microscopy using the Ni-enhanced DAB protocol (Horikawa and Armstrong 1988) using ABC (Avidin-Biotin Peroxidase complex; Vector Laboratories, Burlingame, CA). Digital images were taken by using Adobe PhotoShop with a Kodak M-35 camera attached to the microscope.

### Data analysis

Most analysis was performed by using custom-designed software. The average firing rate during stable EEG states was calculated by averaging spikes per second for at least six 10-s-long periods of artifact-free recording. Pre- and post-stimulus average firing rates were calculated as spikes per second for 10-s periods before and after stimulation. In each case, the mean interspike interval (ISI), standard deviation (SD), standard error of the mean (SE), and the coefficient of variation (CV) were calculated. Whether the changes in unit activity occurred before or after the changes in EEG activity was investigated by correlation analysis. Correlation coefficients were obtained from comparing unit activity against zero-crossings in the EEG signal in a 1-s sliding window moved in 10-ms steps, for intervals of 40 s at a time. The number of spikes was quantified in the same manner along the unit activity track. Correlation coefficients were calculated and the values were plotted. The oscillatory nature of the EEG was investigated by autocorrelograms, and the predominant frequency components were obtained from power spectra calculated using the fast Fourier transform function of the Origin 6.0 software package (Microcal Software, Northampton, MA). The oscillatory nature of the unit activity was investigated by autocorrelograms (Perkel et al. 1967) and Lomb periodograms (Kaneoke and Vitek 1996) of the unit firing. Bursty cells were defined as having a burst index (BI) $\geq$ 0.5 and periods that contained three or more spikes which together, significantly outweighed the number of spikes in other equally long periods in the spike train. Regular and random neurons were defined by BI <0.5. In all cases, the classification was also done according to the shape of the unit firing autocorrelograms (Perkel et al. 1967).

## RESULTS

### Database, selection criteria

From preliminary experiments, in which BF neurons were recorded without EEG monitoring, 47 cells were recovered
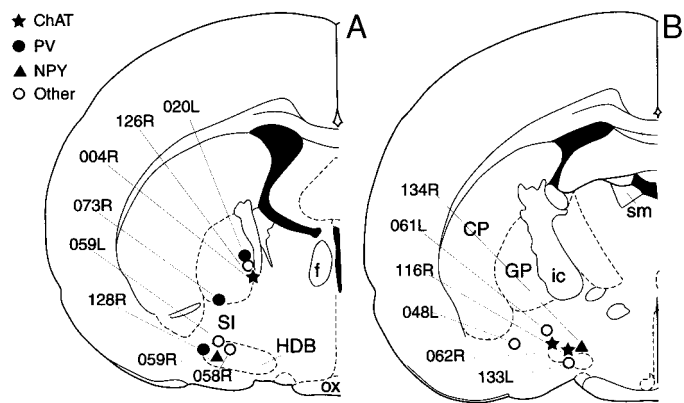


FIG. 2. Rostrocaudal coronal sections depicting the locations of labeled basal forebrain neurons. The numbers represent the designated neuron identification as they appear in all other places of this paper. The symbols represent different types of neurons as indicated in the figure. CP, caudate-putamen; GP, globus pallidus; SI, substantia innominata; HDB, horizontal limb of the diagonal band of Broca; f, fornix; ox, optic chiasm; sm, stria medullaris; ic, internal capsule. *A*: rostral section about −0.8 mm from bregma. *B*: caudal section about −1.3 mm from bregma. Both sections were obtained and modified from the atlas of Paxinos and Watson (1998).
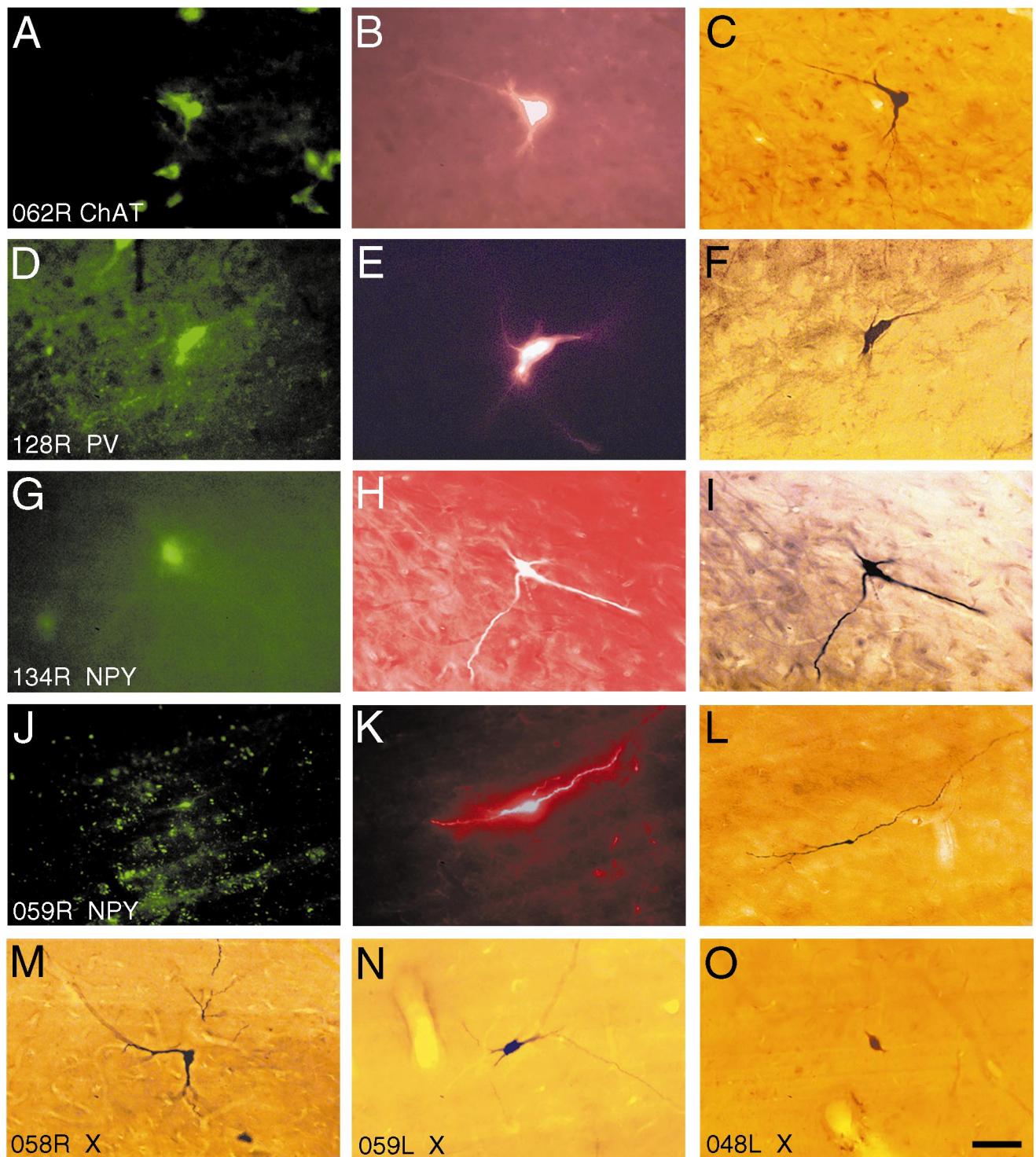
FIG. 3. Photographs of labeled basal forebrain neurons. The 1st 4 rows (*A–L*) depict neurons with identified transmitter. Of these, each row shows the same neuron; the 1st column (*A, D, G, J*) displays the immunocytochemical identification of the neuron using a secondary antibody conjugated to fluorescein isothiocyanate (FITC). The 2nd column (*B, E, H, K*) depicts the single cell juxtacellularly labeled with biocytin and visualized with avidin conjugated lissamine rhodamine. The 3rd column (*C, F, I, L*) shows the neuron developed with nickel enhanced diaminobenzidine (Ni-DAB). The last row (*M–O*) depicts neurons that were negative for both choline acetyltransferase (ChAT) and parvalbumin (PV; labeled ×), developed with Ni-DAB. The numbers correspond to the cell identification. NPY, neuropeptide Y. Scale bar: 50 $\mu$m, applies to all photographs.

successfully (73% success rate) but only 3 cells (*0004R, 073R, 020L*), in which the neurotransmitter content was identified, are included here. In subsequent experiments, 104 BF cells were recorded together with EEG monitoring. Labeling was at-

tempted in 37 of these neurons, of which 29 were recovered successfully (78% success rate). In each case, only a single cell was labeled; 11 cells from this study are reported in this paper, including 5 cells with identified transmitter. From the 11 neu-

rons recorded with EEG, 3 of the cells were observed during both EEG patterns I and II (*128R, 133R, 059L*), 3 neurons were only recorded during pattern II (*116R, 059R, 048L*) and 5 neurons (*062R, 134R, 061L, 058R, 126R*) were recorded exclusively during pattern I.

### Localization and morphology of neurons

From the 14 neurons, 7 were located in the HDB, 4 in the GP along the internal capsule and 3 in the SI. Anatomical localization and immunohistochemical identification of neurons are shown in Fig. 2 and Fig. 3, respectively. Cholinergic neurons (*04R, 062R, 116R*) had triangular-to-round shape cell bodies of $18–25 \times 11–17$ $\mu$m. The thick 3–5 primary dendrites were smooth and gave rise to higher order branches that became varicose, with a few spines. The main axon gave rise to several collaterals bearing very fine en passant varicosities within $0.2–0.3$ mm$^3$ volume around the cell body. PV neurons (*020L, 073R, 128R*) had oval cell bodies of $25–30 \times 8–12$ $\mu$m and usually five or more smooth primary dendrites, which gave rise to higher order branches, in a rather rectangular branching pattern. Distal dendrites became modestly varicose with occasional spines and complex appendage-like endings. Depending on the location, the main axon gave rise to various amounts of local collaterals. One of the NPY cell bodies (*059R*) was small ($8 \times 4$ $\mu$m), oval shaped, with two main dendrites, the other one (*134R*) was large ($30 \times 15$ $\mu$m), multipolar, with five primary dendrites. The axon of the small NPY cell showed numerous local collaterals with irregularly spaced small boutons. In contrast to this, the axon of the large NPY neuron divided into two main branches that were traced as far as the dorsal thalamus and the amygdala, respectively. The axon of this neuron had relatively few local collaterals. Six neurons, which were negative both for ChAT and PV, were characterized by relatively large ($20–27 \times 12–20$ $\mu$m), mostly multi-

polar cell bodies with three to seven generally thick and smooth primary dendrites. Distal dendrites were usually varicose and varied from occasionally spiny to heavily spiny. Since the axons of these neurons could be traced for a relatively long distance with only a few local axon collaterals, we hypothesize that these neurons may represent projection neurons.

### Firing rate and EEG correlation

Analysis of EEG pattern I revealed that unit firing rate increased during spontaneous LVFA when compared with its SWA counterparts in five of eight cases, including *cholinergic neuron 062R* and *PV neuron 128R*. In the other three cells, including the two NPY neurons and *cell 061L,* where NPY staining was not attempted, the LVFA was accompanied by a decrease in firing rate. Firing rates varied considerable, even during the same EEG epochs, ranging between 0 and 12 Hz during SWA and 0 and 22 Hz during the spontaneous LVFA. The average firing rates are shown in Table 1. In all cases, even short temporary changes in the level of cortical activation were matched by a modification in neuronal activity in the BF as shown in parallel changes between the number of zero crossings of the EEG and that of the spikes per second (Fig. 4).

All six cells (*ChAT cell 116R; PV cell 128R, NPY neuron 059R, unidentified cells 048L, 059L; 133L*) recorded during EEG pattern II, fired predominantly during the most active periods of this pattern as evidenced by the spike triggered waveform averages (not shown).

The firing rate changes, during both EEG patterns investigated, were always found to be statistically significant ($P < 0.05$) when 10-s periods before and after stimulation (tail pinch) were compared. However, in many cases (e.g., *062R, 128R, 133L*) the statistical significance was lost when firing rates were averaged at least for 1 min before stimulation (Table 1), and these values were compared with firing rates after tail pinch.

TABLE 1. *Physiological characteristics of identified basal forebrain neurons*

| ID-Transmitter-EEG | Average Firing Rate, spikes/s | | | Rhythmic Frequencies, Hz[a] | Intraburst Frequency, Hz | Firing Pattern[b] | Timing with EEG, ms |
| | PI | PII | Firing Rate TP | | | | |
|---|---|---|---|---|---|---|---|
| *116R*-ChAT-PII | N/A | 14.4 ± 0.22 | N/A | 0.1 | 26.2 ± 1.69 | Bursty | +159 |
| *062R*-ChAT-PI | 5.6 ± 0.23/0.0 | N/A | 5.0 ± 0.01 | N/A | N/A | Random | −405 |
| *004R*-ChAT[c] | 12.2 ± 0.08 | N/A | N/A | N/A | N/A | Random | N/A |
| *128R*-PV-PI, PII | 10.8 ± 1.4/ 2.33 ± 0.79 | 3.5 ± 0.34 | 9.6[d] | 0.74; **2.28** 1.13; **2.12;** 4.5; 8.20 | 14.3 ± 0.3[e] | Bursty/Bursty | −153; +210 |
| *073R*-PV[c] | 14.8 ± 0.49 | N/A | N/A | **1.6** | 15 ± 0.26 | Bursty | N/A |
| *020L*-PV[c] | 40.0 ± 0.44 | N/A | N/A | N/A | N/A | Regular | N/A |
| *134R*-NPY-PI | 0.0/13.1 ± 1.22 | N/A | silent | **1.4; 20.88** | 19.1 ± 0.46 | Bursty | +87 |
| *059R*-NPY-PII | N/A | 0.3 ± 0.02 | silent | N/A | N/A | Random | +40 |
| *061L*-PI | 0.0/6.5 ± 0.76 | N/A | silent | N/A | N/A | Random | +112 |
| *133L*-PI, PII | 4.2 ± 0.43/0.0 | 0.4 ± 0.02 | 3.3 ± 0.74 | N/A | N/A | Random/Bursty | +596; +24 |
| *058R*-PI | 16.3 ± 1.75/ 11.9 ± 0.41 | N/A | 20.6 ± 0.8 5 | **0.4** | 18.3 ± 2.7 | Random | +663 |
| *059L*-PI, PII | 6.7 ± 0.57/ 3.2 ± 0.2 | 4.3 ± 0.58 | 8.3[c] | 0.75; 1.87; **2.19** | 26.4 ± 1.94 | Random/Bursty | −1010; +118 |
| *126R*-PI | 10.7 ± 1.68/ 8.95 ± 1.60 | N/A | N/A | N/A | N/A | Regular | −636 |
| *048L*-PII | N/A | 2.2 ± 0.21 | N/A | 0.4; 0.75 | 6.8 ± 0.60 | Bursty | +446 |

Where applicable, values are means ± SE. Average firing rate for electroencephalographic (EEG) pattern I (PI) is reported for low-voltage fast activity/slow waves, respectively. Values for PI are bold. PII, EEG pattern II; TP, tail pinch; N/A, not applicable; ChAT, choline acetyltransferase; PV, parvalbumin; NPY, neuropeptide Y. [a] Significant peaks in the Lomb periodogram. [b] As defined in METHODS. [c] These units were assumed to be recorded under EEG pattern I. [d] Only two 10-s periods were analyzed. [e] During tail pinch.

## ChAT neuron #062R
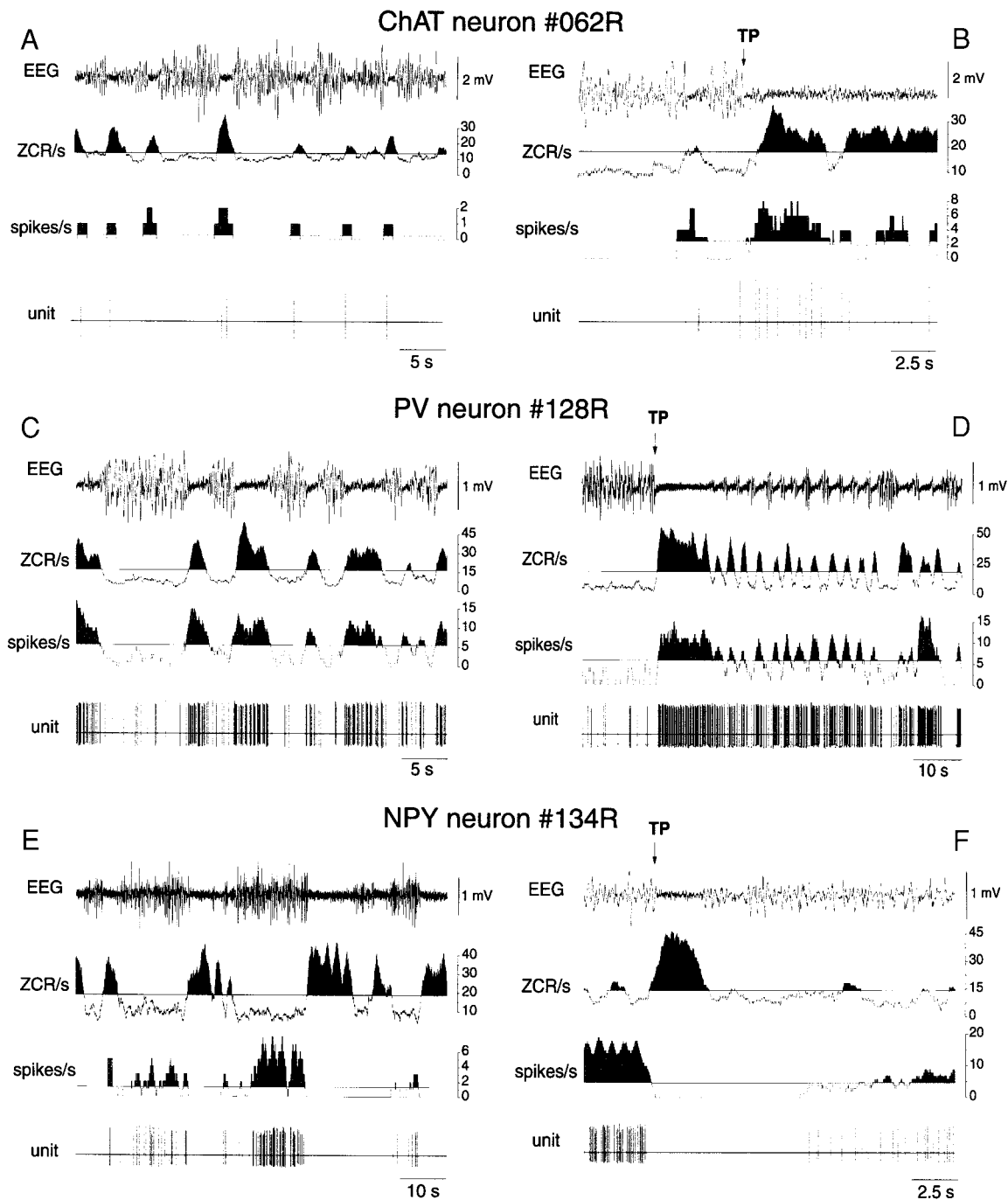


## PV neuron #128R



## NPY neuron #134R



FIG. 4. Unit activity of identified basal forebrain (BF) neurons and its relationship to cortical EEG. In each case, from *top* to *bottom*, EEG shows the electrical activity recorded from the prefrontal/frontal cortex. ZCR/s depicts the histogram of the 0 crossings per second as a means to quantify the wave content of the EEG. Spikes/s shows the histogram of the spikes binned by 1 s overlapping intervals. Areas indicating above the average values are filled in the 2nd and 3rd rows. The 4th row shows the corresponding unit activity from the recorded cell. *Left (A, C, E)*: the unit activity vs. EEG relationship is shown while the EEG changes spontaneously from low-voltage fast activity (LVFA) to slow waves. *Right (B, D, F)*: the corresponding relationship is shown when EEG LVFA is induced by a tail pinch (TP). *A* and *B*: a cholinergic cell that was always firing at a higher frequency during EEG LVFA. *C* and *D*: a parvalbumin-containing cell that also fires at a higher frequency during the EEG LVFA but with a much higher firing rate as compared with the cholinergic cell. *E* and *F*: a neuropeptide Y neuron that always fires at a higher frequency during the EEG slow waves and that stays silent during strong EEG LVFA.

Timing of neuronal and EEG changes was carefully analyzed in both EEG patterns. In EEG pattern I, frequency increase preceded the onset of LVFA in *cholinergic cell 062R*, in PV-containing *neuron 128R* and in one of the cells with unknown transmitter (*126R*). In contrast, in *NPY cell 134R* and

three unidentified neurons (*058R, 133R, 061L*), changes in the unit firing occurred following those in the EEG (Fig. 5, *left*). On the other hand, changes in the unit firing followed the cortical events in all cells analyzed during EEG pattern II (Fig. 5, *right*). In all cases, time lag between neuronal and cortical
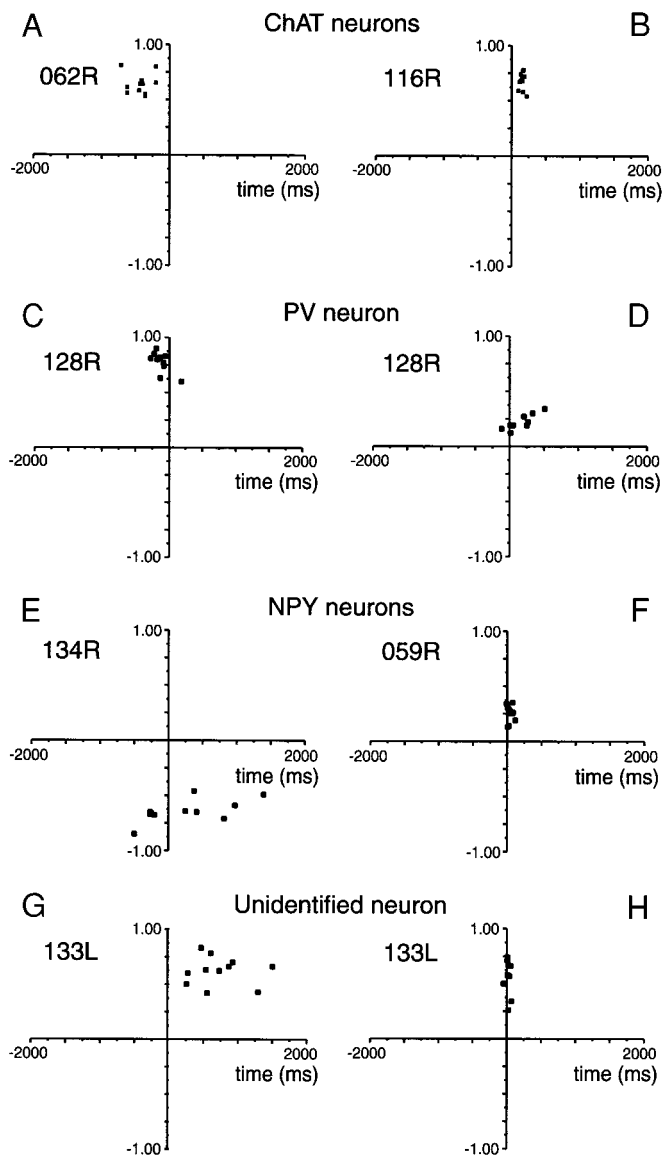
FIG. 5. Plotted correlation coefficients for the 0 crossings vs. the unit firing. Each point corresponds to a 40-s-long period where a 1-s sliding window was used to count the 0 crossings and the corresponding number of spikes. *Left* (*A, C, E, G*): the correlation was calculated while the EEG was in pattern I as shown in Fig. 1*A*. *Right* (*B, D, F, H*): the correlation was calculated while the EEG was in pattern II, as shown in Fig. 1*B*. *A* and *B*: cholinergic neurons. *A*: since all the points are in the upper left quadrant of the correlation vs. time plot, the correlation indicates that the change in unit firing precedes the change in EEG pattern (median = −405 ms). *B*: since all the points are in the upper right quadrant the correlation indicates that the changes in unit firing follow the EEG changes (median = 159 ms). *C* and *D*: PV neuron. As for the previous case, the correlation indicates that the increased firing precedes (median = −153 ms) the change in EEG in pattern I (*C*) while it lags (median = 210 ms) the EEG changes in pattern II (*D*). *E* and *F*: NPY neurons. *E*: because the points are in both the left and the right side of the lower quadrants, the correlation indicates that the unit activity during EEG pattern I can either precede or lag (median = 87 ms) the changes in EEG activity but that in both cases the firing rate is increased during the EEG slow wave activity. *F*: during EEG pattern II, the NPY cell firing occurs lagging the EEG changes (median = 40 ms). *G* and *H*: unidentified neuron. *G*: during EEG pattern I, unit activity lags EEG changes (median = 596 ms), but during EEG pattern II (*H*), the time lag is reduced (median = 24 ms).

changes obtained from the cross-correlograms displayed much less variability and much shorter values during pattern II (usually <100 ms), as indicated by the more compact clustering of

correlation coefficients in Fig. 5. Interestingly, in *PV cell 128R* and *unidentified neuron 059L*, increase of firing rate switched from preceding the EEG changes in pattern I to following them in pattern II (Fig. 5, *C* and *D*).

*Unit firing pattern*

Based on the autocorrelogram (Perkel et al. 1967) of the unit firing and the burst index calculated according to Kaneoke and Vitek (1996), many neurons could be classified as bursty (Table 1); however, this pattern was not unique to any particular class of neurons. Although in EEG pattern I bursts occurred both during LVFA and SWA, in pattern II they often co-occurred with the active dips of the EEG. It was also noticed, that burst firing was usually lost when the EEG switched to a more activated pattern. High-frequency bursts were particularly apparent in *PV cell 128R* and in *NPY cell 134R*.

In half of BF units, grouping of spikes showed rhythmicity. Using the Lomb algorithm, several statistically significant ($P < 0.05$) peaks indicating periodicity of unit discharges were detected (Table 1). For example, in *PV cell 128R* bursts of four to six spikes displayed rhythmicity at ∼2 Hz (intraburst frequency ∼14 Hz) during both spontaneous as well as tail-pinch-induced EEG activation (Fig. 6*B*). With deeper anesthesia, when EEG pattern II was predominant, short pauses in the spike train alternated with short bursts (2–4 spikes, intraburst frequency 50–300 Hz) and single spikes that were separated by 150–250 ms. One of the two low-frequency rhythms that was detected in the Lomb periodogram as a significant peak (1.13 Hz) may correspond to the alternating flat and active periods in the EEG. The other significant peak (4.5 Hz) may correspond to the rhythmic short bursts occurring during the active periods (Fig. 6*A*). *NPY neuron 134R* showed burst firing ∼20 Hz with a superimposed slow rhythm at ∼1.4 Hz (Fig. 6*C*; Table 1). Several neurons displayed rhythmic firing at <1 Hz, including *cholinergic cell 116R*, *PV cell 128R*, and three *unidentified neurons 058R, 059L, 048L*.

DISCUSSION

The close correlation between the timing of changes in the unit firing and the EEG lends support to the previous notion (Metherate et al. 1992) and a recent report (Manns et al. 2000) that BF neurons, including cholinergic cells, play an important role in shaping cortical activation. In addition to cholinergic neurons, the one PV cell that was recorded together with EEG, showed acceleration during activated EEG events. On the other hand, NPY-containing neurons displayed the opposite relationship: these neurons reduced their firing rate during EEG activation.

Data correlating EEG with discharge profiles of nucleus basalis neurons (Buzsaki et al. 1988; Detari and Vanderwolf 1987; Pirch et al. 1986; Szymusiak and McGinty 1989), together with electrophysiological evidence that acetylcholine (ACh) acts as a slow excitatory neurotransmitter in the neocortex (Sillito and Kemp 1983), have been taken as support for the hypothesis that the nucleus basalis provides a steady background of neocortical activity that may enhance the effects of other afferents to the neocortex. Due to the anatomical complexity of the BF, establishment of unequivocal electrophysi-
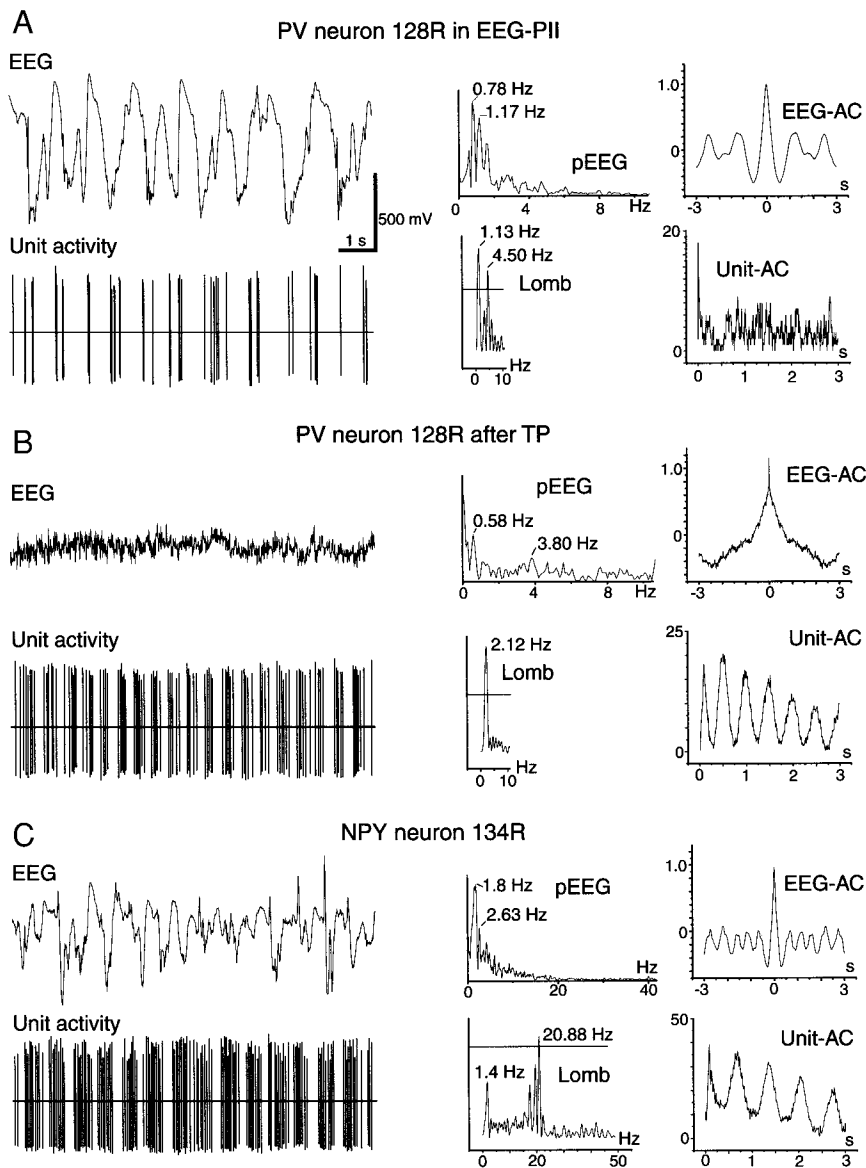
FIG. 6. Spike firing patterns of identified BF neurons in relation to cortical activity during urethan anesthesia. In each case: a 10-s-long EEG trace is shown with the corresponding 10-s-long spike train underneath (unit activity). Scale bars apply to both EEG and unit activity in each case. The corresponding power spectrum of the EEG (pEEG); autocorrelogram of the EEG (EEG-AC); Lomb periodogram of the unit firing (Lomb); and spike autocorrelogram (unit-AC) shown on the *right*. The horizontal line in the Lomb periodograms denotes the significance level of $P = 0.05$. *A*: a PV neuron recorded under EEG pattern II shows $\geq 1$ similar peak of rhythmic activity both in the EEG (1.17 Hz) and the spike train (1.13 Hz), although both spectra also show other rhythms that are not shared. The complex shapes of the EEG-AC and the unit-AC show that there are more than one rhythm present in both cases. Also notice that the unit activity is coincident with the dips of the EEG waves that correspond to the high-frequency components of this pattern. *B*: the same neuron after stimulation has now become more rhythmic as shown by the Lomb periodogram (peak at 2.12 Hz) and also by the very periodic unit-AC. However, the rhythmicity seems to be independent of the cortical activity since there is no similar peak seen in the pEEG. *C*: an NPY-positive neuron whose unit activity is very rhythmic, as evidenced by the periodic shape of unit-AC, and with a significant periodicity at ~20 Hz, as shown in the Lomb periodogram. This periodicity is not found in the EEG, which, however, displays rhythmicity in the delta band, as shown in the pEEG and EEG-AC.

ological signatures of the different basal forebrain neurons would enormously facilitate clarification of the role played by this area in the regulation of cortical activity. Although initial studies reported heterogeneity in the antidromic latencies of basalocortical neurons, a proper assignment of these data to cholinergic or GABAergic neuronal populations was equivocal due to the lack of chemical identification of the recorded neurons (Aston-Jones et al. 1985; Detari and Vanderwolf 1987; Reiner et al. 1987). According to the in vitro finding by Alonso et al. (1996), cholinergic neurons possess a low-voltage Ca-mediated burst mechanism, while noncholinergic cells lack it but show a rhythmic clustered spike discharge. A recent study described that the majority of cholinergic neurons shifted from a tonic or irregular discharge to a robust rhythmic bursting pattern in response to tail-pinch-induced stimulation (Manns et al. 2000). However, they also noted that cholinergic neurons did not differ physiologically from some of the noncholinergic cells that display low-frequency rhythmicity.

In our smaller sample, however, cholinergic neurons did not show robust bursting during spontaneous or stimulation-in-

duced EEG activation. Moreover, burst firing was not characteristic for any cell type identified in our study. Furthermore the stimulation-induced rhythmic burst firing of a PV neuron in our study was remarkably similar to the cholinergic neurons described by Manns et al. (2000). Although our study investigated very closely the temporal relationship between unit firing and EEG, cholinergic neurons were in the same category as PV and unidentified neurons that increased their firing preceding changes of the EEG. These findings indicate that a more extensive database of identified cells is needed before electrophysiological criteria can be used to reliably distinguish different BF cell types.

In earlier studies reporting EEG-related changes in neuronal activity in the BF, most of the cells were found to have higher firing rate during fast cortical activity, hence termed F cells (Detari and Vanderwolf 1987; Detari et al. 1997; Dringenberg and Vanderwolf 1998). Our finding, that the firing of *PV neuron 128R* had a strong positive correlation with EEG activation indicates that there are also PV cells among the F cells. PV has been found in GABAergic neurons in many brain areas,

including GABAergic local neurons of the cerebral cortex, the neostriatum, and septohippocampal projection neurons (Celio 1990; Kita et al. 1990). Since GABAergic basalocortical axons were found to terminate exclusively on cortical GABAergic interneurons (Freund and Meskenaite 1992), our finding is compatible with the notion that at least a subpopulation of PV-containing basalocortical neurons promotes functional activation in the cerebral cortex by disinhibition (Jimenez-Capdeville et al. 1997).

In addition to neurons that increased their firing during cortical activation, several studies described the presence of a smaller number of BF cells that reduced their firing during EEG activation (Detari et al. 1997; Manns et al. 2000). These latter, so called S cells were thought to be local interneurons, as they could not be activated antidromically from the cortex, and it was suggested that they may be GABAergic neurons inhibiting cholinergic cells (Detari et al. 1997). On the other hand, Szymusiak and McGinty (1986, 1989) described some BF cells in cat that increased their discharge in anticipation of NREM sleep onset. These "sleep active" neurons were antidromically driven from the external capsule and cingulate bundle and were tentatively identified as either cholinergic (Szymusiak and McGinty 1986) or GABAergic neurons (McGinty and Szymusiak 1990). To our knowledge, this is the first report to positively identify NPY neurons as they relate to EEG. The two NPY neurons recorded in this study were strongly inhibited by strong mechanical stimulation, and this was unique to this cell type. According to our partial reconstruction, the axon of *NPY neuron 059R* displayed a massive local arborization, giving rise to ~600 local boutons. Since local NPY axons have been described innervating cholinergic neurons (Tamiya et al. 1991; Zaborszky 1989; Zaborszky and Duque 2000) and NPY neurons are colocalized with GABA in the forebrain (Aoki and Pickel 1989), it is likely that NPY neurons could profusely affect cortical EEG via the cholinergic corticopetal neurons. The other NPY neuron (*134R*) did not display abundant local axon-collaterals but was characterized by a long bifurcating axon that was traced as far as the dorsal thalamus, confirming studies in rodents (Hallanger et al. 1987), cats, and monkeys (Parent et al. 1988) that BF neurons innervate thalamic nuclei. A previous tracer study (Asanuma and Porter 1990) in rat described that at least part of this BF-thalamic projection is GABAergic; our data, in agreement with these studies, would raise the possibility that at least some cells in the BF that contain NPY would affect cortical activity via the thalamus.

Steriade et al. (1993) described in acutely prepared animals a novel slow cortical rhythm characterized by alternating depolarized and hyperpolarized epochs in the pyramidal cells with a frequency of 0.3–1.0 Hz. This rhythm was later confirmed in naturally sleeping animals (Steriade 1996) and also in humans (Amzica and Steriade 1997) and is likely to be generated by the cortex as supported by data showing that this rhythm persists in thalamectomized and brain-stem-transected preparations (Steriade et al. 1993) and vanishes in subcortical structures after cortical inactivation (Magill et al. 2000). The slow oscillations are important in controlling the coherence of spindles and delta waves, two other sleep-related oscillations that are generated in the thalamo-cortical circuitry (Steriade 1999).

Based on the presence of rhythmic patterns with similar frequencies both in BF cholinergic neurons and in the EEG during noxious stimulation, it was claimed by Jones and her coworkers (Maloney et al. 1997; Manns et al. 2000) that slow and high-frequency rhythms could be transmitted to cortical fields via ascending basalo-cortical fibers during particular behaviors and states. Although in EEG pattern II peaks in the Lomb periodogram were often matched with similar peaks in the EEG power spectrum, this was not the case in more active EEG patterns. Indeed, our study, which investigated the correlation between BF firing and EEG in more physiological conditions, including well-characterized spontaneous EEG epochs as well as after brief stimulation, suggests a more complex scenario.

The frequency decomposition of the EEG showed in EEG pattern I peaks in the beta and delta frequencies, but in pattern II the peak frequency band was compressed ~1 Hz (Fig. 6). Also the average unit firing rate, across all neurons except the NPY cells, was significantly higher (6.9 vs. 2.6 Hz) during EEG pattern I than pattern II, suggesting that the underlying mechanisms of these two patterns may be different. At present, it is unknown where such generalized patterns are initiated; however, our data showing that in pattern I changes started in BF cells earlier than in pattern II, are compatible with the hypothesis that pattern I is generated by BF cells and/or transmitted from the brain stem via the BF to the cortex. On the other hand, our finding that all units recorded under EEG pattern II showed delayed increased firing in relation to cortical activation suggests that under this state, cortical activation may be transmitted via descending corticofugal fibers to the BF (Zaborszky et al. 1997). A treatise that considers a dynamic interplay within BF as well as between BF and other brain circuitries rather than assuming a unidirectional process (Manns et al. 2000) is more compatible with a previous suggestion of the role of diffuse brain stem versus restricted telencephalic input to BF neurons (Zaborszky et al. 1991, 1999) and with recent theories about the role of the BF in arousal and attentional mechanisms (Sarter and Bruno 2000).

Our findings clearly show that monitoring of EEG-related BF neuronal activity combined with chemical identification of the recorded neurons is a very promising approach for clarifying its role in the regulation of cortical activity. However, the proper interpretation of the data requires adding knowledge about the synaptic connections of the identified neurons.

## REFERENCES

ALONSO A, KHATEB A, FORT P, JONES BE, AND MUHLETHALER M. Differential oscillatory properties of cholinergic and noncholinergic nucleus basalis neurons in guinea pig brain slice. *Eur J Neurosci* 8: 169–182, 1996.

AMZICA F AND STERIADE M. The K-complex: its slow (1-Hz) rhythmicity and relation to delta waves. *Neurology* 49: 952–959, 1997.

AOKI C AND PICKEL VM. Neuropeptide Y in the cerebral cortex and the caudate-putamen nuclei: ultrastructural basis for interactions with GABAergic and non-GABAergic neurons. *J Neurosci* 9: 4333–4354, 1989.

ASANUMA C AND PORTER LL. Light and electron microscopic evidence for a GABAergic projection from the caudal basal forebrain to the thalamic reticular nucleus in rats. *J Comp Neurol* 302: 159–172, 1990.

ASTON-JONES G, SHAVER R, AND DINAN TG. Nucleus basalis neurons exhibit axonal branching with decreased impulse conduction velocity in rat cerebrocortex. *Brain Res* 325: 271–285, 1985.

BUZSAKI G, BICKFORD RG, PONOMAREFF G, THAL LJ, MANDEL R, AND GAGE FH. Nucleus basalis and thalamic control of neocortical activity in the freely moving rat. *J Neurosci* 8: 4007–4026, 1988.

CELIO MR. Calbindin D−28k and parvalbumin in the rat nervous system. *Neuroscience* 35: 375–475, 1990.

DETARI L, RASMUSSON DD, AND SEMBA K. Phasic relationship between the activity of basal forebrain neurons and cortical EEG in urethane-anesthetized rat. *Brain Res* 759: 112–121, 1997.

DETARI L, RASMUSSON DD, AND SEMBA K. The role of basal forebrain neurons in tonic and phasic activation of the cerebral cortex. *Prog Neurobiol* 58: 249–277, 1999.

DETARI L AND VANDERWOLF CH. Activity of identified cortically projecting and other basal forebrain neurones during large slow waves and cortical activation in anaesthetized rats. *Brain Res* 437: 1–8, 1987.

DRINGENBERG HC AND VANDERWOLF CH. Involvement of direct and indirect pathways in electrocorticographic activation. *Neurosci Biobehav Rev* 22: 243–257, 1998.

FREUND TF AND MESKENAITE V. Gamma-aminobutyric acid-containing basal forebrain neurons innervate inhibitory interneurons in the neocortex. *Proc Natl Acad Sci USA* 89: 738–742, 1992.

GRAHN DA, RADEKE CM, AND HELLER HC. Arousal state vs. temperature effects on neuronal activity in subcoeruleus area. *Am J Physiol* 256: 840–849, 1989.

GRITTI I, MAINVILLE L, AND JONES BE. Codistribution of GABA- with acetylcholine-synthesizing neurons in the basal forebrain of the rat. *J Comp Neurol* 329: 438–457, 1993.

HALLANGER AE, LEVEY AI, LEE HJ, RYE DB, AND WAINER BH. The origins of cholinergic and other subcortical afferents to the thalamus in the rat. *J Comp Neurol* 262: 105–124, 1987.

HORIKAWA K AND ARMSTRONG WE. A versatile means of intracellular labeling; injection of biocytin and its detection with avidin conjugates. *J Neurosci Methods* 25: 1–11, 1988.

JIMENEZ-CAPDEVILLE ME, DYKES RW, AND MYASNIKOV AA. Differential control of cortical activity by the basal forebrain in rats: a role for both cholinergic and inhibitory influences. *J Comp Neurol* 381: 53–67, 1997.

KANEOKE Y AND VITEK JL. Burst and oscillation as disparate neuronal properties. *J Neurosci Methods* 68: 211–223, 1996.

KITA H, KOSAKA T, AND HEIZMANN CW. Parvalbumin-immunoreactive neurons in the rat neostriatum: a light and electron microscopic study. *Brain Res* 536: 1–15, 1990.

KORKMAZ S AND WAHLSTROM G. The EEG burst suppression threshold test for the determination of CNS sensitivity to intravenous anesthetics in rats. *Brain Res Brain Res Protoc* 1: 378–384, 1997.

MAGILL PJ, BOLAM JP, AND BEVAN MD. Relationship of activity in the subthalamic nucleus-globus pallidus network to cortical electroencephalogram. *J Neurosci* 20: 820–833, 2000.

MALONEY KJ, CAPE EG, GOTMAN J, AND JONES BE. High-frequency gamma electroencephalogram activity in association with sleep-wake states and spontaneous behaviors in the rat. *Neuroscience* 76: 541–555, 1997.

MANNS ID, ALONSO A, AND JONES BE. Discharge properties of juxtacellularly labeled and immunohistochemically identified cholinergic basal forebrain neurons recorded in association with the electroencephalogram in anesthetized rats. *J Neurosci* 20: 1505–1518, 2000.

MCGINTY D AND SZYMUSIAK R. Keeping cool: a hypothesis about the mechanisms and functions of slow-wave sleep. *Trends Neurosci* 13: 480–487, 1990.

METHERATE R, COX CL, AND ASHE JH. Cellular bases of neocortical activation: modulation of neural oscillations by the nucleus basalis and endogenous acetylcholine. *J Neurosci* 12: 4701–4711, 1992.

NUNEZ A. Unit activity of rat basal forebrain neurons: relationship to cortical activity. *Neuroscience* 72: 757–766, 1996.

PANG K, TEPPER JM, AND ZABORSZKY L. Morphological and electrophysiological characteristics of noncholinergic basal forebrain neurons. *J Comp Neurol* 394: 186–204, 1998.

PARENT A, PARE D, SMITH Y, AND STERIADE M. Basal forebrain cholinergic and noncholinergic projections to the thalamus and brainstem in cats and monkeys. *J Comp Neurol* 277: 281–301, 1988.

PAXINOS G AND WATSON C. *The Rat Brain in Stereotaxic Coordinates.* New York: Academic, 1998.

PERKEL DH, GERSTEIN GL, AND MOORE GP. Neuronal spike trains and stochastic point processes. I. The single spike train. *Biophys J* 7: 391–418, 1967.

PINAULT D. A novel single-cell staining procedure performed in vivo under electrophysiological control: morpho-functional features of juxtacellularly labeled thalamic cells and other central neurons with biocytin or Neurobiotin. *J Neurosci Methods* 65: 113–136, 1996.

PIRCH JH, CORBUS MJ, RIGDON GC, AND LYNESS WH. Generation of cortical event-related slow potentials in the rat involves nucleus basalis cholinergic innervation. *Electroencephalogr Clin Neurophysiol* 63: 464–475, 1986.

REINER PB, SEMBA K, FIBIGER HC, AND MCGEER EG. Physiological evidence for subpopulations of cortically projecting basal forebrain neurons in the anesthetized rat. *Neuroscience* 20: 629–636, 1987.

SARTER M AND BRUNO JP. Cortical cholinergic inputs mediating arousal, attentional processing and dreaming: differential afferent regulation of the basal forebrain by telencephalic and brainstem afferents. *Neuroscience* 95: 933–952, 2000.

SILLITO AM AND KEMP JA. Cholinergic modulation of the functional organization of the cat visual cortex. *Brain Res* 289: 143–155, 1983.

STERIADE M. Awakening the brain. *Nature* 383: 24–25, 1996.

STERIADE M. Coherent oscillations and short-term plasticity in corticothalamic networks. *Trends Neurosci* 22: 337–345, 1999.

STERIADE M, AMZICA F, AND CONTRERAS D. Cortical and thalamic cellular correlates of electroencephalographic burst-suppression. *Electroencephalogr Clin Neurophysiol* 90: 1–16, 1994.

STERIADE M, NUNEZ A, AND AMZICA F. A novel slow (1 Hz) oscillation of neocortical neurons in vivo: depolarizing and hyperpolarizing components. *J Neurosci* 13: 3252–3265, 1993.

SZYMUSIAK R AND MCGINTY D. Sleep-related neuronal discharge in the basal forebrain of cats. *Brain Res* 370: 82–92, 1986.

SZYMUSIAK R AND MCGINTY D. Sleep-waking discharge of basal forebrain projection neurons in cats. *Brain Res Bull* 22: 423–430, 1989.

TAMIYA R, HANADA M, INAGAKI S, AND TAKAGI H. Synaptic relation between neuropeptide Y axons and cholinergic neurons in the rat diagonal band of Broca. *Neurosci Lett* 122: 64–66, 1991.

ZABORSZKY L. Afferent connections of the forebrain cholinergic projection neurons, with special reference to monoaminergic and peptidergic fibers. In: *Central Cholinergic Synaptic Transmission,* edited by Frotscher M and Misgeld U. Birkhauser: Basel, 1989, vol. 57, p. 12–32.

ZABORSZKY L, CULLINAN WE, AND BRAUN A. Afferents to basal forebrain cholinergic projection neurons: an update. *Adv Exp Med Biol* 295: 43–100, 1991.

ZABORSZKY L AND DUQUE A. Local synaptic connections of basal forebrain neurons. *Behav Brain Res.* In press.

ZABORSZKY L, GAYKEMA RP, SWANSON DJ, AND CULLINAN WE. Cortical input to the basal forebrain. *Neuroscience* 79: 1051–1078, 1997.

ZABORSZKY L, PANG K, SOMOGYI J, NADASDY Z, AND KALLO I. The basal forebrain corticopetal system revisited. *Ann NY Acad Sci* 877: 339–367, 1999.